ChemComm

Accepted Manuscript

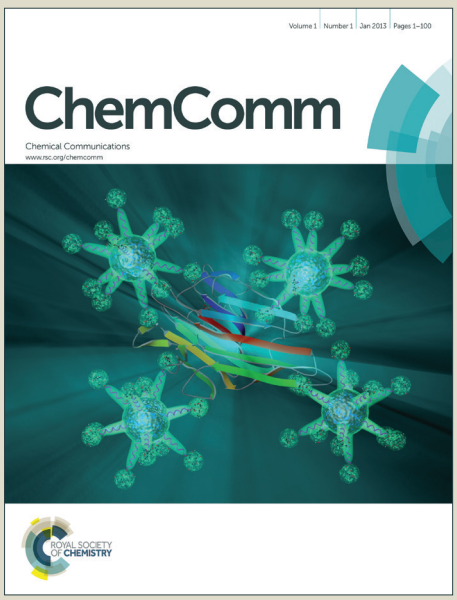

ROYAL SOCIETY OF CHEMISTRY

www.rsc.org/chemcomm

Journal Name

COMMUNICATION

Not all Density Functionals are Created Equal: The Case of the Missing Electron in the Oxidized $[W–W{\equiv}O]^{7+}$ Core

Received 00th January 20xx,
Accepted 00th January 20xx

DOI: 10.1039/x0xx00000x

www.rsc.org/

David W. Brogden[a] and John F. Berry[a,b]

The location of the unpaired electron in the new mixed-valent $(W_2)^{IV,V}$ trication $[W_2O(dpa)_4]^{3+}$ presents a challenge for DFT methods. EPR spectroscopy confirms the unpaired electron to be in the W(V)-oxo unit, in agreement with the predictions of hybrid functionals B3LYP and TPSSh, but contrary to the predictions of non-hybrid functionals.

Compounds with weak metal-metal interactions provide challenging problems for theory.[1-8] A classic example is the case of quadruply-bonded Cr_2 tetracarboxylate and related compounds, for which the Slater determinant corresponding to the $\sigma^2\pi^4\delta^2$ quadruple bond typically contributes to only < 50% of the ground state wavefunction, causing Hartree-Fock (HF)-derived computational methods to fail.[9, 10] We recently reported a novel complex with a linear W···W≡O geometry, $[W_2O(dpa)_4]^{2+}$ (**1**), (dpa = 2,2′-dipyridylamido) shown in Scheme 1,[11, 12] that provides an electronic structure problem of an entirely different nature. The very weak W···W σ bonding interaction in the compound leads to an electronic structure that can be approximated as containing two distinct weakly interacting W(IV) centers.[12] Because of the differing geometries of the two W centers (W(1) is ligated by eight N atoms in a rough square antiprismatic geometry, while W(2) is square pyramidal bearing four equatorial N atoms and an apical terminal oxo group), each W(IV) atom is expected to have a different HOMO. As is typical for square pyramidal terminal oxo complexes, W(2) has a $(d_{xy})^2$ electron pair. W(1), on the other hand, has an electron pair in the d_z2 orbital (Scheme 1), which has slight contributions from W(2) and the oxo ligand due to the weak W–W–O three-center σ interaction in the compound.[12] One issue that was only partially settled in our previous work is the question of whether the W(1) d_z^2 orbital or the W(2) d_{xy} orbital is highest in energy for the compound. Density functional theory (DFT) calculations, with the BP86 functional, that we have reported on this complex indicated that these two orbitals are very close to each other in energy, < 0.1 eV.

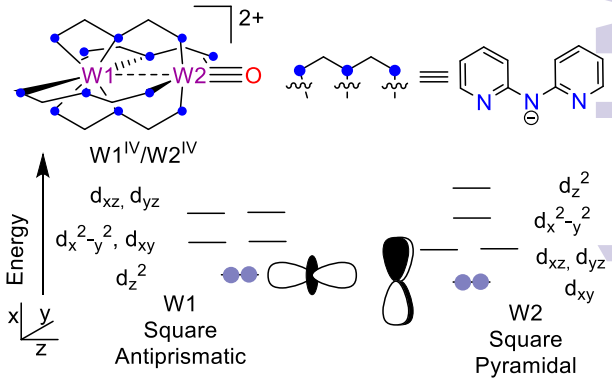

Scheme 1. Representation of **1** and molecular orbital diagram for the individual W(IV) centers.

In order to settle this question of the orbital ordering in the W···W≡O complex, we present here an experimental/computational approach in which we have (1) chemically synthesized a new, isostructural, one-electron oxidized analog of **1**, namely, $[W_2O(dpa)_4]^{3+}$ (**2**), (2) characterized the environment of its unpaired electron by EPR spectroscopy, and (3) used various DFT methods to calculate the electronic structure of **2**. DFT calculations on **2** are highly functional-dependent, and care must be taken in the analysis of the computational results in order to find the correct ground state.

Since the W(1) d_z^2 orbital is involved in small but significant σ bonding delocalization throughout the W–W=O chain, we may expect removal of an electron from this orbital yielding what is hereafter referred to as electron configuration 1 (EC1) to cause a lengthening of the W–W bond distance, as well as the W=O bond distance. On the other hand, the W(2) d_{xy} orbital is essentially non-bonding with respect to both the W–W and the W=O interaction. Therefore, we may not expect to see a large change in the W–W or W=O distances from **1** to **2** if electron configuration 2 (EC2) is adopted, in which an electron is removed from the W(2) d_{xy} orbital.

Having the possibility of two distinct electron configurations at two different W–W distances in **2** is the equivalent of setting up a booby trap for quantum chemical calculations, as a geometry optimization routine can readily fall into a local, and not a global, potential energy minimum. We therefore decided to use several different den-

[a] Department of Chemistry, University of Wisconsin-Madison, 1101 University Ave. Madison, WI
[b] Email: berry@chem.wisc.edu

functionals to probe the potential energy landscape of the W–W distance of **2** using relaxed surface scans. For this work, we use the GGA functional BP86, and the meta-GGA TPSS, as well as hybrid versions of each one (B3LYP and TPSSh, respectively), that include HF exchange. Notable is that all four of these functionals provide an accurate optimized geometry for the diamagnetic complex **1**, with a possible exception of B3LYP, which overestimates the W–W distance by 0.07 Å (See Table S1). Surface scans of the W–W distance of **2** with each functional are shown in Figure 1,[†] where the W–W distances have been scanned from 2.9 – 3.4 Å, in both directions from the original W–W distance in **1**, 3.07 Å.

Surprisingly, both BP86 and its hybrid counterpart B3LYP show a single minimum in their scans (Figure 1 a, b) corresponding to wildly different W–W distances of ~ 3.3 and 3.1 Å, respectively. TPSS and TPSSh also show significant differences in the predicted equilibrium W–W distance, but now in each case the scans (Figure 1 c, d) show the expected two minima. However, TPSS predicts the minimum with the longer W–W distance to be lower in energy, while TPSSh shows a clear preference for the shorter W–W distance. Interestingly, the GGA functionals do not predict double-well minima, while the meta-GGA functionals do. Also, EC1 is predicted by non-hybrid functionals while the hybrid functionals predict an EC2 ground state. In previous computational work on metal-metal bonded compounds, we have consistently found that non-hybrid functionals provide a more reliable description of the ground state.[9, 13, 14] Thus, we are curious which prediction, a long or short W–W distance for **2**, is in best agreement with experiment in this case.

The trication **2** was synthesized by reaction of **1** with two equivalents[‡] of Ag(OTf), (OTf = trifluoromethanesulfonate) in dichloromethane at 0 °C, and crystals suitable for X-ray crystallography were grown by slow diffusion of hexanes into a dichloromethane solution at –20 °C. In the crystal structure of **2** at 100 K, the asymmetric unit is found to contain one W–W=O species, three triflate anions, and one dichloromethane solvent of crystallization. Thus, the

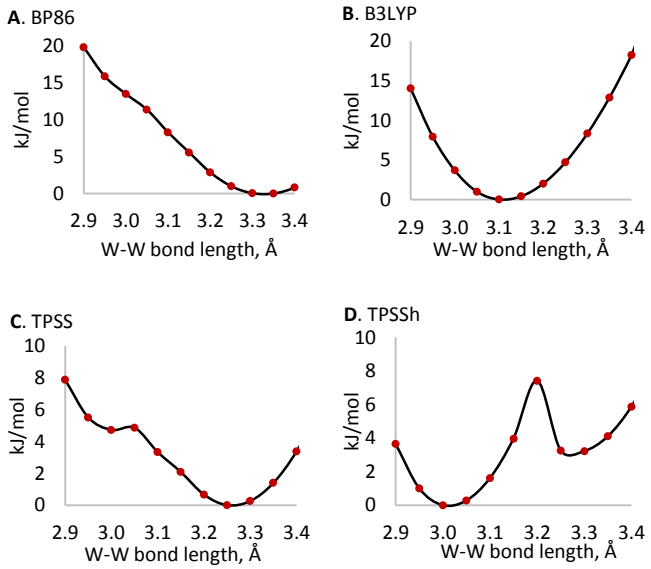

Figure 1. Potential energy surface scans for **2** with the (A) BP86 functional, (B) B3LYP functional, (C) TPSS functional, (D) TPSSh functional with fixed W–W bond distance from 2.9 to 3.4 Å.

stoichiometry is consistent with the presence of a $[W_2O(dpa)_4]$ tricationic unit, as expected for **2**. The $[W_2O(dpa)_4]^{3+}$ ion, shown in Figure 2, bears significant similarity to the structure of **1** in that houses two chemically distinct W atoms, one ligated by eight dpa N atoms, and the other ligated by four dpa atoms bearing a terminal oxo group. There are, however, some unusual and unexpected features: The W···W distance in **2** is 2.9719(2) Å, which is ~0.1 Å shorter than the W···W distance in **1**. Also, while **1** features a near linear W–W=O unit with a W–W=O angle of 178°, the W–W=O unit in **2** is distinctly bent, with a W–W=O angle of 168.78(8)°. Changes in all of the W–N bond distances from **1** to **2** are minimal, ~0.02 Å in the largest case, so it is difficult to judge from these data whether oxidation is localized on one W center vs the other. Nevertheless, in comparison to our expectations for EC1 vs EC2, the change in the W W distance seems inconsistent with an EC1 ground state.

This sentiment is matched by poor agreement between optimized geometries for **2** at the BP86 or TPSS levels and its crystal structure (Table 1), where the calculated W–W distances are > 0.2 Å too long. Improved optimized geometries are obtained with the hybrid functionals B3LYP and especially TPSSh. The latter predicts not only a W–W distance of 3.017 Å, but also a bent W–W=O unit with an angle of 174°. It is worth noting that the TPSSh functional is the only functional to predict a non-linear W–W=O angle, though the energy associated with W–W=O bending is on the order of only a few kJ/mol according to DFT results. The close correspondence of the experimental crystal structure data and the structure predicted by TPSSh suggests that upon oxidation a d_{xy} electron from the oxo bound tungsten atom is lost. Figure 3 shows a plot of this orbital as well as the W(1) d_{z^2} orbital, calculated by the TPSSh functional. Complex **2** therefore has an unpaired electron in the W(V)-oxo $5d_{xy}$ orbital, and there is a closely-lying electron pair in the $5d_{z}2$ orbital of the distal W atom that shows partial electron delocalization to the W(V)-oxo unit, Table S2, as indicated by the calculated W–W Mayer bond order of 0.45. This dative W(IV)→W(V) interaction is likely the reason for the unexpected non-linearity of the W–W≡O angle as well as the shorter W–W distance in **2** vs **1**, since the W(V) will be a stronger Lewis acidic center. The W≡O bond is elongated by this dative metal-metal interaction, but only by < 0.01 Å as compared to the structure of **1**. Consistent with this view, the W=O

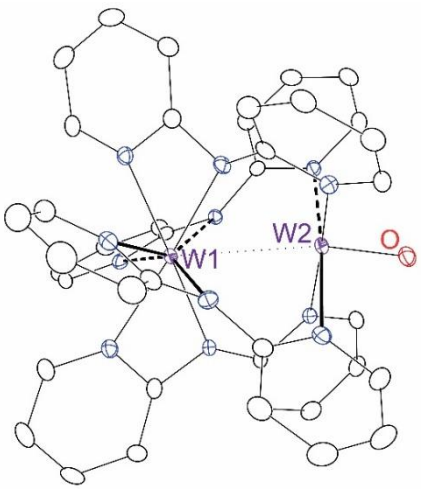

Figure 2. X-ray crystal structure of the trication in **2**, with thermal ellipsoids drawn at the 50% probability level. Hydrogen atoms, solvent molecules, and counter ions have been omitted for clarity.

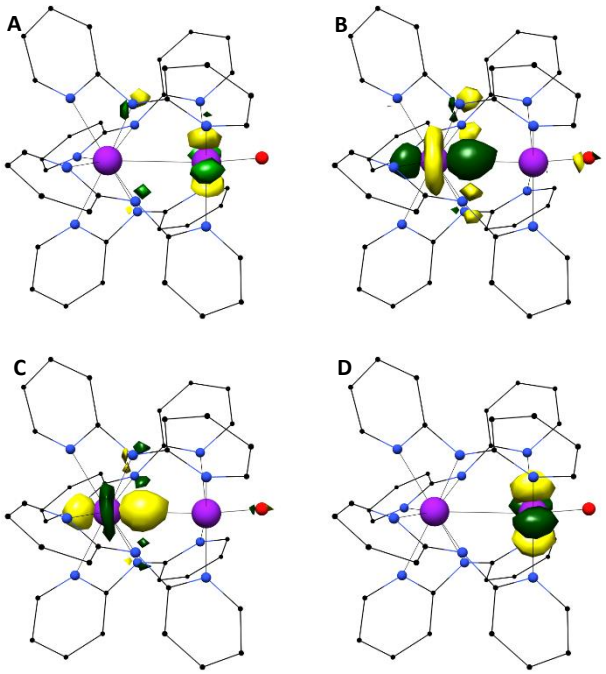

Figure 3. (A) Alpha HOMO-1 d_{xy} molecular orbital. (B) Alpha HOMO d_{z^2} molecular orbital. (C) Beta HOMO d_{z^2} molecular orbital. (D) Beta LUMO d_{xy} molecular orbital. All orbitals calculated with the TPSSh functional.

stretch for **2** is found at 955 cm^{-1}, as compared to 957 cm^{-1} in **1**. In an attempt to validate this electronic structure further, a low temperature EPR spectrum of **2** was collected to characterize the location of the unpaired electron.

The EPR spectrum collected on a frozen solution of **2** (8 K), shown in Figure 4, is nearly isotropic in character, but is best simulated with an axial *g* tensor in which all three *g* components are less than 2, g_1 = 1.818, g_2 = 1.836, g_3 = 1.836. The low *g* values are characteristic for W(V)-oxo metal centers with a $(d_{xy})^1$ electron configuration.[15-18] ^{183}W hyperfine coupling is mainly unresolved in the spectrum, but is best modeled by (isotropic) A values that are larger for one W atom than they are for the other, consistent with the hypothesis that the unpaired electron is mainly localized on the W=O unit. The experimental data in combination with the good agreement between the calculated geometric parameters of **2** by the TPSSh functional indicate that the oxidized compound of **1** adopts EC2, where indeed the unpaired electron is in the oxo bound tungsten d_{xy} orbital, resulting in a mixed-valent W(IV)-W(V)-oxo species.

Compounds containing both metal-metal and metal-ligand multiple bonding interactions have been shown to engage in extraordinary chemical reactivity.[19-25] Recently, **1** was shown to react with alkyl phosphines in CH_3CN not by O-atom transfer, but instead via single-electron transfer (SET) causing a cascade of radical reactions leading ultimately to the hydration of CH_3CN.[11] Although little work has been reported on the reactivity of mononuclear W(V)-oxo compounds,[26] it is reasonable to expect **2** to show similar reactivity to **1**, but perhaps

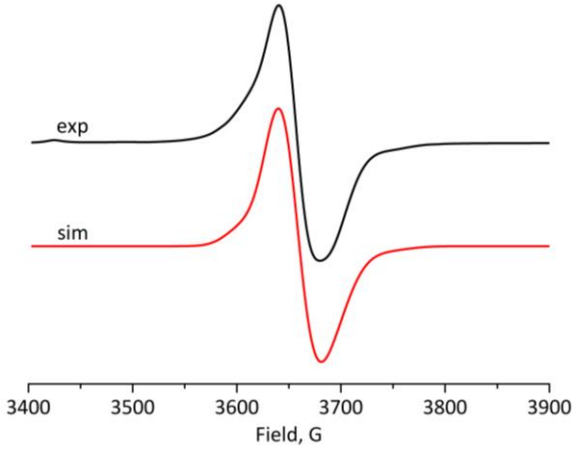

Figure 4. EPR data and simulation for $[W_2O(dpa)_4]^{3+}$ (**2**) at 8 Simulation parameters are as follows: freq = 9.38; g = (1.818, 1.836 1.836); A = (0, 0, 0; 170, 170, 300); HStrain = (70, 70, 100); lw – points = 4096.

Table 1. X-ray and DFT calculated bond distances and bond angles for **2**.

	W–W, Å	W–O, Å	W_{oxo}–N, avg. Å	$W_{dist.}$–N_a, avg. Å	W_{dist}–N_{py}, avg Å	W–W-O, °
2	2.971 9(2)	1.697(2)	2.140[3]	2.162[3]	2.183[3]	168.78(8)
TPSSh	3.017	1.692	2.147	2.178	2.207	173.9
B3LYP	3.107	1.685	2.157	2.199	2.227	179.8
TPSS	3.243	1.684	2.153	2.185	2.212	179.9
BP86	3.312	1.685	2.141	2.163	2.207	179.9

with greater scope due to its higher oxidation state. Indeed, reactions of **2** with excess tri-*tert*-butylphosphine (P^tBu_3) and tri-*n*-butylphosphine (P^nBu_3) in acetonitrile show similar results to those reported for **1**. In dichloromethane, **2** was reduced by these substrates to **1** and then showed no further reactivity. Expanding the scope of this reactivity, both **1** and **2** also react in CH_3CN with Me_2PhP and Ph_2MeP, again via SET. Compound **2** also undergoes SET with PPh_3 and methyl *p*-tolyl sulphide to form **1**, whereas **1** does not react with these substrates. Overall, **2** is more oxidizing than **1** and is, to our knowledge, the first example of a W(V)-oxo complex that engages in SET in the presence of O-atom acceptors.

Reported here is the first example of a W(V)-oxo complex that has a second W(IV) ion is its immediate vicinity. The electronic structure of this complex has provided a challenge for DFT methods, and we have found the combination of a meta-GGA functional with hybrid HF character was needed in order to provide an accurate prediction of its geometry and ground state features. This compound features a highly unusual dative W(IV)→W(V)≡O interaction in its electronic structure that accounts for its unusual geometrical features, and facilitates unusual SET reactivity with phosphine and sulfide substrates.

Notes and references

[†] The GGA functionals PBE and PBE0 have also been tested and their surface scans are given in Figure S1.

‡ The second equivalent of Ag(OTf) is needed to provide the correct stoichiometric equivalents of the (OTf) counter anion.

We thank the NSF for Grant CHE-100464. DFT calculations were supported by the NSF under Grant CHE-0840494.
Electronic Supplementary Information (ESI) available: Experimental and theoretical details, figures and tables. See DOI: 10.1039/x0xx00000x

1. F. A. Cotton, Murillo, C. A., Walton, R. A., ed., *Multiple Bonds Between Metal Atoms*, Springer US, New York, 2005.
2. B. O. Roos, A. C. Borin and L. Gagliardi, *Angew. Chem. Int. Ed.*, 2007, **46**, 1469-1472.
3. C. J. Cramer and D. G. Truhlar, *Phys. Chem. Chem. Phys.*, 2009, **11**, 10757-10816.
4. F. Neese, *Coord. Chem. Rev.*, 2009, **253**, 526-563.
5. F. Ruipérez, J. M. Ugalde and I. Infante, *Inorg. Chem.*, 2011, **50**, 9219-9229.
6. K. P. Kepp, *Coord. Chem. Rev.*, 2013, **257**, 196-209.
7. L. R. Falvello, B. M. Foxman and C. A. Murillo, *Inorg. Chem.*, 2014, **53**, 9441-9456.
8. A. C. Tsipis, *Coord. Chem. Rev.*, 2014, **272**, 1-29.
9. G. Li Manni, A. L. Dzubak, A. Mulla, D. W. Brogden, J. F. Berry and L. Gagliardi, *Chem. Eur. J.*, 2012, **18**, 1737-1749.
10. M. B. Hall, *Polyhedron*, 1987, **6**, 679-684.
11. M. Nippe, S. M. Goodman, C. G. Fry and J. F. Berry, *J. Am. Chem. Soc.*, 2011, **133**, 2856-2859.
12. D. W. Brogden, Y. Turov, M. Nippe, G. Li Manni, E. A. Hillard, R. Clérac, L. Gagliardi and J. F. Berry, *Inorg. Chem.*, 2014, **53**, 4777-4790.
13. G. H. Timmer and J. F. Berry, *Chem. Sci.*, 2012, **3**, 3038-3052.
14. G. H. Timmer and J. F. Berry, *C. R. Chim.*, 2012, **15**, 192-201.
15. K. M. Stobie, Z. R. Bell, T. W. Munhoven, J. P. Maher, J. A. McCleverty, M. D. Ward, E. J. L. McInnes, F. Totti and D. Gatteschi, *Dalton Trans.*, 2003, 36-45.
16. L. E. Bevers, P.-L. Hagedoorn and W. R. Hagen, *Coord. Chem. Rev.*, 2009, **253**, 269-290.
17. G. Nandi and S. Sarkar, *Eur. J. Inorg. Chem.*, 2013, **2013**, 3518-3525.
18. G. Nandi and S. Sarkar, *Inorg. Chim. Acta*, 2014, **410**, 106-110.
19. J. F. Berry, *J Chem Sci*, 2015, **127**, 209-214.
20. K. P. Kornecki, J. F. Berry, D. C. Powers and T. Ritter, in *Progress in Inorganic Chemistry Volume 58*, John Wiley & Sons, Inc., 2014, pp. 225-302.
21. J. F. Berry, *Dalton Trans.*, 2012, **41**, 700-713.
22. K. P. Kornecki, J. F. Briones, V. Boyarskikh, F. Fullilove, J. Autschbach, K. E. Schrote, K. M. Lancaster, H. M. L. Davies and J. F. Berry, *Science*, 2013, **342**, 351-354.
23. A. R. Corcos, A. K. M. Long, I. A. Guzei and J. F. Berry, *Eur. J. Inorg. Chem.*, 2013, **2013**, 3808-3811.
24. A. K. M. Long, G. H. Timmer, J. S. Pap, J. L. Snyder, R. P. Yu and J. F. Berry, *J. Am. Chem. Soc.*, 2011, **133**, 13138-13150.
25. A. K. Musch Long, R. P. Yu, G. H. Timmer and J. F. Berry, *J. Am. Chem. Soc.*, 2010, **132**, 12228-12230.
26. W. A. Nugent and J. M. Mayer, *Metal-Ligand Multiple Bonds: The Chemistry of Transition Metal Complexes Containing Oxo, Nitrido, Imido, Alkylidene, or Alkylidyne Ligands*, John Wiley & Sons, 1988.

